

Synthesis and characterization of polymeric responsive CMC/Pectin hydrogel films loaded with *Tamarix aphylla* extract as potential wound dressings

BARKAT ALI KHAN¹; FAZAL KARIM¹; MUHAMMAD KHALID KHAN^{1,*}; FAHEEM HAIDER¹; SADIQUILLAH KHAN²

¹ Drug Delivery and Cosmetics Laboratory, Gomal Center of Pharmaceutical Sciences, Faculty of Pharmacy, Gomal University, D.I. Khan, 29050, Pakistan

² Department of Environmental Science, Faculty of Engineering & Technology, Gomal University, D.I. Khan, 29050, Pakistan

Key words: *Tamarix aphylla*, Hydrogel film, Burn wound, Carboxymethyl cellulose, Pectin

Abstract: The fourth most predominant overwhelming type of trauma is burn injuries worldwide. Ideal wound healing dressings help in the wound healing process in a lower time with less pain. Commonly used dry wound dressing, like absorbent gauze or absorbent cotton, possess limited therapeutic effects and require repeated use, which further exaggerates patients' suffering. In contrast, hydrogels films present a promising alternative to improve healing by guaranteeing a moisture balance at the wound site. The aim of the current study was to synthesize *Tamarix aphylla* (*T. aphylla*) extract-loaded hydrogel film with Na-CMC and pectin and to study their wound healing properties. The Na-CMC/Pectin hydrogels films were synthesized and characterized for HPLC analysis, FTIR, surface morphology, rheology, tensile strength, swelling behavior, drug release kinetics, and *in vivo* wound healing in an animal model. FTIR confirmed the existence of strong interaction between both polymers but no interaction with the extract. SEM photographs showed successful embedding of extract in small pores of hydrogel film and showed smooth and homogenous morphology. Rheological and texture profiles indicated that hydrogels behaved as strong gels. Swelling and erosion were dependent on the amount of the CMC. HPLC showed drug content of three selected formulation (A3, E3 and S3) as $85 \pm 0.1\%$, $82.5 \pm 0.4\%$ and $80 \pm 0.3\%$, respectively. The release of the drug from the hydrogel was controlled by a Fickian diffusion mechanism. *In vivo* wound healing activity of hydrogel film confirmed that *T. aphylla* extract successfully promoted healing rate by significantly reducing ($P < 0.05$) the size of wound closure compared to the control group, evidenced by intensive collagen formation in histopathological and biochemical analysis. The capability of these hydrogels for burn wounds could be valuable for medical uses as a new window of safe and effective medication.

Introduction

A wound may be defined as the breaking or the loss of anatomic and cellular or functional connection of living tissue (Kased *et al.*, 2017). It is an unavoidable part of human life that is caused by chemical, physical, thermal, immunological, or microbial damages to the tissue (Mehmet *et al.*, 2020a). Wound closure represents a primary goal in the treatment of deep and large wounds, for which the mortality rate is predominantly high. Spontaneous adult skin healing eventually results in the formation of epithelialized scars, which cause life-long deformities. Thus,

it can be suggested that wound closure by skin regeneration instead of repair should be the primary goal of burn wound management (Mishra *et al.*, 2008; Ghorpade *et al.*, 2017; Elegbede *et al.*, 2020).

The traditional concept of temporary wound dressings is increasingly replaced by novel drug delivery systems like polymeric scaffolds (hydrogels), which can promote healing by regeneration phenomenon (Diez-Pascual and Diez-Vicente, 2015). Hydrogels as polymeric drug delivery systems have presented one of the most convincing areas of research and significant scope for researchers in drug delivery systems (Khan *et al.*, 2020; Hoffman, 2012). They have been classified as three-dimensional swellable hydrophilic polymeric networks that have the ability to absorb an adequate amount of water or aqueous solution, thus triggering them to swell (Ballesteros *et al.*, 2018; Annabi *et al.*, 2014). Hydrophilic groups impart swelling

*Address correspondence to: Muhammad Khalid Khan, khalid.gomalian@gmail.com.

Received: 09 December 2020; Accepted: 03 February 2021



behavior to the hydrogel while cross-linking plays role in the mechanical strength of hydrogels. Hydrogels have excellent resemblance with living tissues because of their tendency to become rubbery soft when they are in the swollen state (Annabi *et al.*, 2014; Kibar and Us, 2013). Researchers have been using different natural polymers, such as pectin, alginate, and chitosan for the production of hydrogels. Their wide application in the fabrication of wound dressing is based on their similitude to the extracellular matrix, which further improves acceptance by biological systems through the inhibition of the immunological reactions frequently observed for synthetic polymers (Caló and Khutoryanskiy, 2015; Peck *et al.*, 2009). It is suggested by the biomaterial scientists that hydrogels are ideal dressing membranes for wound healing and suitable applicants for patients with burn wounds (Girard *et al.*, 2007). They can be applied as a permanent or temporary dressing for different wounds to support the regeneration and healing of the injured skin (Martelli *et al.*, 2017; Kased *et al.*, 2017).

Despite recent advances in wound care products, traditional therapies based on natural origins, such as plant extracts are interesting alternatives that had been used in ancient times to accelerate the wound healing process (Huang *et al.*, 2019a). These therapies offer new possibilities for the treatment of skin diseases, enhancing access to healthcare and allowing overcoming some limitations associated with the modern products and therapies, such as the high costs, the long manufacturing times, and the increase in bacterial resistance (Bibi *et al.*, 2015; Huang *et al.*, 2019b). *Tamarix aphylla*, also known as *Athel*, *Abel*, *Ghaz*, and *Saltcedar* is natively cultivated in Africa and the Middle East but with wide geographical distribution, extending from Australia to the United States. It is a perennial tree, innate across East, North, and Central Africa, over the Middle East, and found in many parts of southern and Western Asia (Han *et al.*, 2013). Several studies have recognized the various types of secondary metabolites present in *T. aphylla*. Reports had identified the presence of polyphenols, flavonoids, saponins, coumarins, tannins, triterpenes, and alkaloids in the bark of *T. aphylla* (Jasim and Albazaz, 2019; Alhourani *et al.*, 2018). Traditionally, it has been used as folk medicine, usually to cure different pathological conditions and ailments, including liver inflammation, skin disorders, and wound healing (Ebid, 2015; Han *et al.*, 2013; Alhourani *et al.*, 2018). Nevertheless, only a few studies have focused on investigating the plant's wound healing activity in animal models by incorporating its extract in polymeric hydrogels.

The aim of this research was to provide a concise insight on the key properties of hydrogel for wound healing and regeneration by delivering natural products as a safe and effective medication.

Materials and Methods

Plant sample

A well-developed big trunk of *T. aphylla* was selected for bark collection. It was verified by a taxonomist from the Department of Biological Science, Gomal University, D. I. Khan, Pakistan, and a voucher specimen was deposited.

The reference no. is 578/PS-GU/2019. The bark was washed with water and ground using pestle and mortar for coarse powder and then in an electric grinder for fine powder. Finally, the fine powder was stored in polythene bags for further processing. Extraction was carried out as per the protocols of Bibi *et al.* (2015) using 400 g of *T. aphylla* bark powder in 2 L of 70% ethanol with continuous stirring. The yield was 18% on a w/w basis (Bibi *et al.*, 2015).

Chemicals and reagents

Carboxy methyl cellulose (Na-CMC 1500-3000 high viscosity) and Pectin were purchased from Sigma Aldrich, USA. Citric acid was purchased from Merck, Germany. Monobasic potassium phosphate (KH₂PO₄), sodium hydroxide (NaOH), and 95% ethanol were purchased from BDH England.

Hydrogel synthesis

The hydrogel films were prepared according to a study reported with slight modification (Ali *et al.*, 2018; Barkat *et al.*, 2020). Na-CMC was dissolved in double-distilled water (Solution A) in a beaker and placed on a hot plate stirrer at 80°C for 1 h until a clear solution was obtained, while pectin was also dissolved in double-distilled water (Solution B) in a separate beaker and placed on a hot plate. Solutions A and B were mixed for 2 h with continuous heat on a hot plate magnetic stirrer. Then citric acid was first dissolved in a specific quantity of water and filled in 1 mL of a syringe. NaCMC/Pectin solution was placed on a magnetic stirrer, and citric acid was slowly poured drop wise via syringe. *T. aphylla* bark extract (15%) was used by dissolving in 70% ethanol and mixed with NaCMC/Pectin solution. After complete mixing, distilled water was added in sufficient quantity to the mixture to make the final weight 100 g (c). Solution (40 g) was cast in two Petri dishes and kept at room temperature for 24 h and then placed in an oven at 60°C for the next 24 h. After 48 h the thin hydrogel films were dried and removed from Petri dishes with the help of a cutter. The hydrogel films were wrapped in aluminum foil and kept in polythene bags. Tab. 1 shows the concentration of different ingredients that are used in the preparation of CMC/Pectin hydrogel films.

Characterizations of hydrogel films

HPLC analysis

HPLC (Perkin Elmer, USA) system was attached with detector and C-18 column having dimension 250 mm × 4.6 mm, 5 μm (Supelco USA) were available in NPRL lab and used for this study. The mobile phase consists of 0.1 M acetic acid (Solvent A) and acetonitrile (Solvent B). The elution time of the sample was 5 min and 6 min subsequent washing of column before injection of next sample. The flow rate and injection volumes were 1 mL/min and 10 μL, respectively. The sample was filtered via syringe filter and chromatograms were recorded at 270 nm (Bao *et al.*, 2011).

Swelling study

The degree of swelling of CMC/Pectin hydrogel film was investigated by the method used by Bao *et al.* Phosphate buffer of pH (1.2, 5.5, and 7.4) was used for swelling studies. For this purpose, a piece of hydrogel film of about (3 × 3 cm) was weighted initially (W_i) and then placed in a specific buffer

TABLE 1

Composition of hydrogel films (W/W)

Formulations	NaCMC/Pectin (wt% ratio)	Na-CMC(g)	Pectin (g)	Citric acid (g)	Citric acid (wt% of NaCMC)	<i>T. aphylla</i> extract (g/g)
A1	50/50	0.5	0.5	10	0.05	1.6
A2	100/50	1	0.5	10	0.10	1.6
A3	75/25	1.5	0.5	10	0.15	1.6
E1	100/80	1	0.8	10	0.10	1.6
E2	50/50	1	1	10	0.10	1.6
E3	100/120	1	1.2	10	0.10	1.6
S1	100/50	1	0.5	15	0.15	1.6
S2	100/50	1	0.5	20	0.20	1.6
S3	100/50	1	0.5	25	0.25	1.6

solution for 8 h. After 8 h, each hydrogel film was blotted on tissue paper in order to remove the excess water, and then the final weight (W_f) was measured. The value was put in the below-mentioned equation in order to find out the swelling percentage of CMC/Pectin hydrogel film. The experiment was performed in triplicate, and results were averaged.

$$\text{Swelling degree (\%)} = (W_f - W_i)/W_i \times 100 \quad (1)$$

where W_i is the initial weight before swelling and W_f is the final weight after swelling.

Mechanical properties

The mechanical strength of the hydrogel films was examined under ambient conditions using a Texture analyzer (Testometrics UTS, United Kingdom). Five rectangular-shaped strips of 2 cm width and 5 cm length were cut from each of the hydrogel formulations and were held between the grips of the machine. The initial grip separation and cross-head speed were set to 50 mm and 5 mm/min, respectively. The sample was stretched with a force of about 50 N. Force applied with which sample breaks was recorded. The test was conducted in triplicate, and results were averaged (Rachtanapun *et al.*, 2012).

Fourier transform infrared spectroscopy (FTIR)

The selected CMC/Pectin hydrogel film was characterized by FTIR analysis (UATR TWO, Perkin Elmer, UK) to evaluate cross-linking between the polymers initiated by citric acid. For this purpose, powder of Na-CMC, pectin, citric acid, dried bark extract powder of *T. aphylla*, and extract loaded CMC/pectin hydrogel film was selected and subjected to analysis. Each sample was placed on crystal and scanned in the range of 4000–400 cm^{-1} . The analysis was performed three times, and calculations were made to get the average of results (Ramli and Wong, 2011).

Scanning electron microscopy (SEM)

The surface morphological characteristics of the optimized CMC/Pectin hydrogel films were determined with the help of Scanning Electron Microscopy (TESCAN Vega LMU, UK). The specific acceleration voltage was 30 kV, and the magnification power was 50 \times . The samples were pre-coated with gold before subjected to scanning (Alam *et al.*, 2017).

Drug content analysis

The specific quantity of the drug that was loaded in hydrogel film was quantified by dissolving the hydrogel in ethanol on a magnetic stirrer for 24 h. The drug leached out from the film, and then this amount of drug was calculated using HPLC (Perkin Elmer, USA) (Hemant *et al.*, 2016).

Weight uniformity

Hydrogel film was cut into a specific dimension (3 \times 3 cm), and then its dry weight was measured by using a weighing balance. This test was performed six times, and results averaged with standard deviation were noted.

In vitro drug release

Three formulations A3, E3, and S3 of hydrogel were subjected to the drug release experiment. For this purpose, Franz diffusion cell was used. During release studies, a semipermeable membrane was fixed between the donor and receiving chambers of the Franz diffusion cell. Buffer pH 7.4 was placed in receiving chamber in order to mimic the skin environment. At time 0, 0.5, 1, 2, 4, 8, 12, 16, 20, and 24 h, the sample was taken from receiving chamber and replaced with an equal amount of buffer solution to maintain the sink condition. The aliquot was examined by using high-performance liquid chromatography (Liu *et al.*, 2018).

Kinetic equation

Weibull model was applied to release data; it describes the stored fraction of drug 'm' in solvent at time t .

$$F = 1 - e^{(-at^b)} \quad (2)$$

where a represents the time parameter, which is time-dependent process. T_i is the location parameter and represents the lag time before release process and mostly it will be zero. b describes the shape of dissolution curve.

In vivo studies

Ethical approval

In vivo/animal experimentation was performed according to rules and regulations of the departmental/institutional ethical committee of Gomal University, D.I. Khan under reference ERB/GU/14-2019.

Animals selection

Male rabbits, with weights that ranged from 1.5 to 2 kg, were selected for wound healing purposes. A total of 15 male rabbits were used, which were divided into 3 groups: experimental, standard, and blank groups, containing 5 rabbits each. Animals were kept in proper environmental conditions having access to food and water.

Induction of wounds in animals

Wounds were created in rabbits following the already reported procedure of Yusufoglu and Alqasoumi (2011). Animals were anesthetized with ketamine and xylazine mixture, and hairs were removed from the back of the rabbits using an electronic trimmer. Thermal injury was created by fitting a metal rod on the shaved area. Melted wax was introduced into the metal rod (heated at 80°C). After 10 min, the metal rod with wax was removed from the back of the animal. In this way, a 2nd-degree burn wound was created in the animal skin, which was confirmed by observing redness, swelling, and inflammation at the site of the wound. The diameter of the wound was dependent on the diameter of the metal rod, which was approximately 20 mm.

Treatment protocols

Group I: Treated with CMC/Pectin hydrogel film containing *T. aphylla* extract (Experimental group). *Group II:* Treated with a marketed product (Burnol®, Eufavin) (Standard group). *Group III:* Treated with blank hydrogel (Control group).

Wound size measurement

Wound dimensions were determined with the help of image-J software. Control and treated groups were properly analyzed for the wound size at fixed days such as day 0, 7, 14, and 21 days. The healing percentage on a certain day was the difference between the initial wound (in day zero) and the healing wound on that day. The percentage of wound closure was examined by using the following equation:

$$\% \text{Wound Closure} = \frac{\text{wound area on day } 0 - \text{Wound area on day } n}{\text{wound area on day } 0} \times 100 \quad (3)$$

where n is the number of days (7th, 14th and 21st days).

The wound diameter was assessed using transparent meter rule. The wound area was determined by the following formula

$$\text{Area} = \pi r^2$$

where r^2 = diameter of wound and $\pi = 22/7$.

The area was measured and recorded as the initial area of the wound (wound area at day 0). The percentage wound contraction of each rabbit was determined, and the average was calculated for each group.

Histopathological analysis

The histopathology of wounds was performed according to the previously reported studies using hematoxylin and eosin (H&E) staining techniques with slight modifications (Ashraf et al., 2018; Towfiq et al., 2015). On the 21 days of treatment, the newly formed wound tissue was carefully excised from the rabbits of all groups. The wound tissues were fixed in formalin solution (10%), which were sectioned at 4 μm . The sections were then stained with hematoxylin and eosin. Using

a light microscope, the stained tissues were assessed for re-epithelization, vascularity, and fibroblast content.

Biochemical analysis

Biochemical analysis was performed to check the level of hydroxyproline and hexosamine in the wounded area of all the animal groups. For this purpose, hydroxyproline and hexosamine were estimated by the method used by Woessner (1961). Briefly, the wound tissues were dried using a vacuum drier at a temperature of $125 \pm 5^\circ\text{C}$. It was then exposed to HCl (6 N) at $125 \pm 5^\circ\text{C}$ for 3 h, neutralized to pH 6.8, and subjected to chloramine-T oxidation for 20 min. Ehrlich reagent was used to develop the color after the addition of perchloric acid (0.04 M) solution. Using a digital photoelectric colorimeter (Wincom®, AE-11D, China), the light transmission was determined at 557 nm. The hexosamine was determined by hydrolyzing the dried wound tissues in 6 N HCL at $100 \pm 5^\circ\text{C}$ for 8 h, which was neutralized to pH 7 with 4 N sodium hydroxide (NaOH) and diluted with water. The diluted solution was mixed with acetylacetone and heated up to $95 \pm 5^\circ\text{C}$ for 45 min. This solution was then cooled, and ethanol (95%) and Ehrlich reagent were added. After thorough mixing for an hour, the absorbance was determined at 530 nm using a digital photoelectric colorimeter (Elegbede et al., 2020).

Statistical analysis

Data were expressed as means and standard deviation (S.D). Collected data were analyzed using the two-way ANOVA to determine the effects of treatment and time. SPSS statistical package (SPSS, Version 15.0, Chicago, ILL, USA) was used for the analysis of the data. Values of less than 5% ($P < 0.05$) were considered to be significant.

Results and Discussion

HPLC analysis

Eight different peaks were identified because of various active phytochemicals present in the *T. aphylla* extract. According to the literature, phenols and polyphenols include *p*-coumaric, gallic and ellagic acids, and flavonoids compounds composed of mono-methyl ether and poly-methyl ether quercetin derivatives are present in *T. aphylla* extract (Yusufoglu and Alqasoumi, 2011; Akhlaq and Mohammed, 2011). HPLC standard and reference chromatogram of *T. aphylla* bark extract are shown in Fig. 1.

Swelling studies

Swelling data of different hydrogel film formulations are presented in Fig. 2. In the first three formulations (A1, A2, and A3), the concentration of Na-CMC increased from 0.5 to 1 and 1.5 g, respectively. When these hydrogel formulations were exposed to different pH for swelling studies, swelling increases from acidic range (1.2) to slightly acidic range (5.5) and finally becomes maximum at neutral pH (7.4). By increasing the amount of Na-CMC, the swelling percentage also increases (Ortega-Toro et al., 2014; Sutar et al., 2008). The reason was that because Na-CMC is a hydrophilic polymer and rapidly swells in phosphate buffer pH 7.4. The swelling of CMC/Pectin hydrogel was

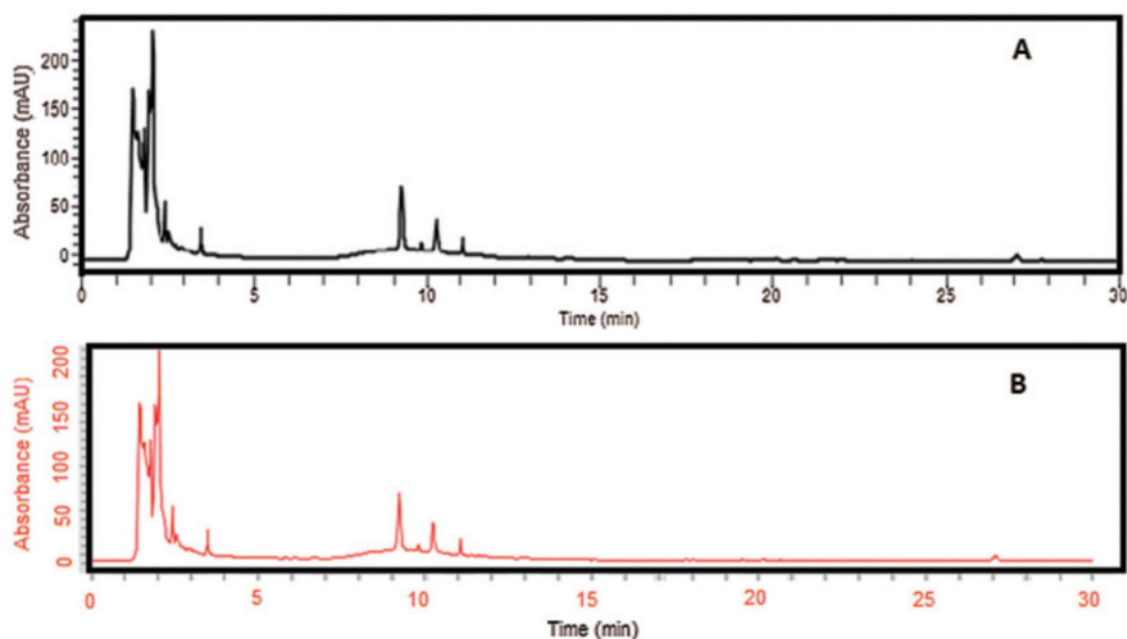


FIGURE 1. (a) HPLC Chromatograms of crude ethanolic extract of *T. aphylla*. (b) Extract loaded in hydrogel film analyzed at 270 nm.

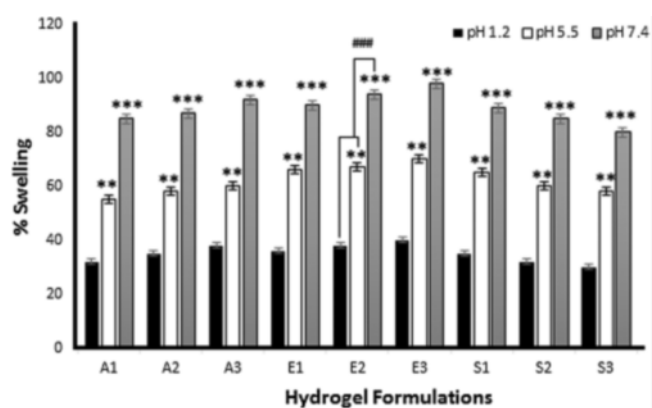


FIGURE 2. Percent swelling of hydrogel films at different pH 1.2, 5.5, and 7.4. The data is presented as the mean \pm SD and analyzed using ANOVA. ** $P < 0.01$ and *** $P < 0.001$ refers to statistical significance of both pH (5.5 and 7.4) from pH 1.2.

pH-dependent and is fully controlled by a H-bond formed by the loss of (H^+) of the COOH group present in Na-CMC. Generally, the COOH group ionizes at alkaline pH, which causes deprotonation in the solution, so at pH 7.4, the above-mentioned group bearing negative charge on the polymer chain, which is responsible for self-repulsion and hence more swelling of hydrogel film was achieved (Ghorpade *et al.*, 2017). Formulations E1, E2, and E3 composed of varying concentrations of pectin (0.8, 1, and 1.2 g) in CMC/Pectin hydrogel film, respectively, are shown in Tab. 1. The same pattern was observed as in the case of Na-CMC. By increasing the amount of Pectin in hydrogel formulation, the swelling rate was boosted. Hydrogel film showed maximum swelling ratio at pH 7.4 and lowest swelling at lower pH 1.2. The reason was that pectin is a water-soluble polymer and readily swells at pH 7.4 (Kibar and Us, 2013). S1, S2, and S3 CMC/Pectin hydrogel film formulation in which citric acid concentration was varied from 0.15, 0.2, and 0.25 g, respectively. Although all these formulations exhibited

maximum swelling at pH 7.4, a reverse behavior was observed with citric acid concentration. The results depicted that by enhancing the amount of cross-linker the swelling rate was down regulating. This was actually due to tightening the polymeric structure, which strongly entanglement the chains of the polymer, as a result, swelling of CMC/Pectin hydrogel film was diminished (Tong *et al.*, 2008).

Mechanical properties

Tensile strength is an important physicochemical characteristic of dressing materials. Dressing materials must be tough and elastic and withstand different conditions like storage, transportation, and application at the wound site. Fig. 3a shows the effect of Na-CMC on the tensile strength of CMC/Pectin hydrogel film. The results showed that by increasing the concentration of Na-CMC, the mechanical strength of CMC/Pectin hydrogel film was decreased. Fig. 3b represents the impact of Pectin on the tensile strength of CMC/Pectin film. By increasing the pectin, the tensile strength of CMC/Pectin hydrogel film was increased. Fig. 3c displayed the effect of citric acid (cross-linker) on the hydrogel. By increasing the amount of cross-linker the tensile strength of the film was enhanced due to the strong cross-linking effect produced between the polymeric chains which ultimately increased the mechanical properties of hydrogel film (Kibar and Us, 2013; Tong *et al.*, 2008).

ATR-FTIR of hydrogel film

ATR-FTIR spectrum of polymers and their active and inactive ingredients of CMC/Pectin hydrogel film was presented in Fig. 4. Fig. 4a shows the spectra of Na-CMC powder, in which the hydrophilic region showed its band at 3352.10 cm^{-1} , symmetric alkyl chain appeared at 2896 cm^{-1} , carbonyl group appeared at 1587.76 cm^{-1} , 1416.6 , and 1052.6 representing OH stretching in plane and C-O stretching, respectively (Burki *et al.*, 2020). The FTIR of pectin (Fig. 4b) shows an absorption band at 3365.20 cm^{-1} ,

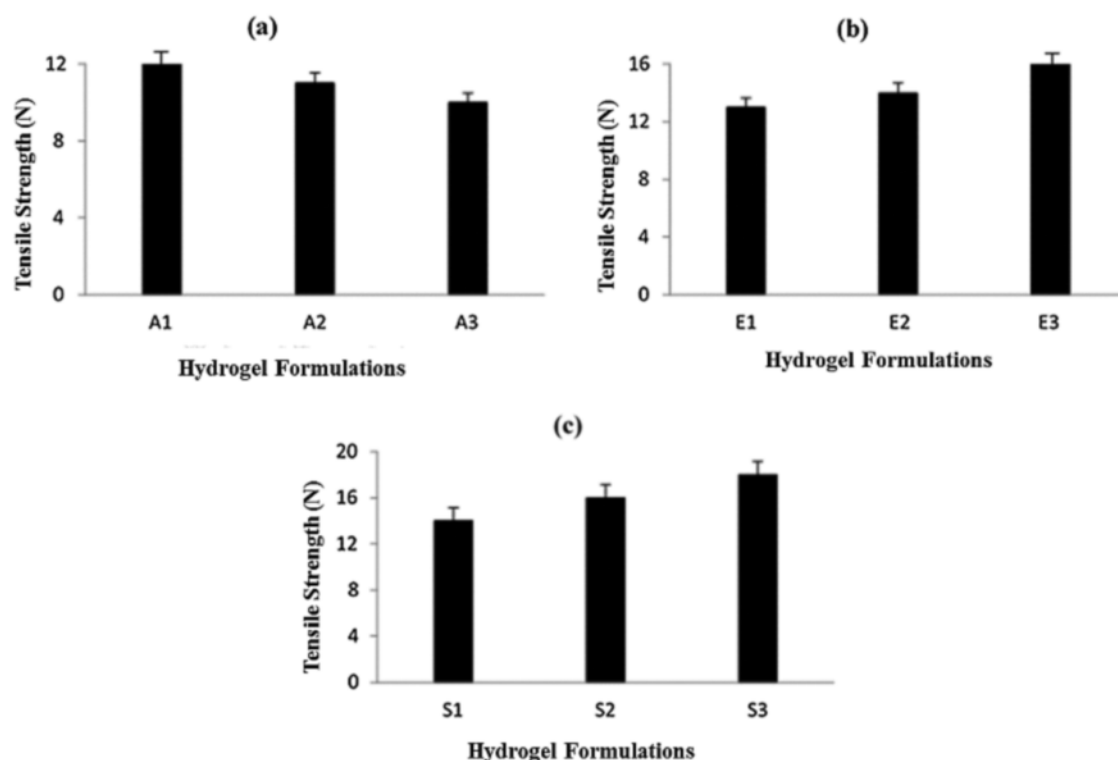


FIGURE 3. (a) Effect of Na-CMC on hydrogel film (b) Effect of pectin on hydrogel film (c) Effect of citric acid cross-linker on hydrogel film.

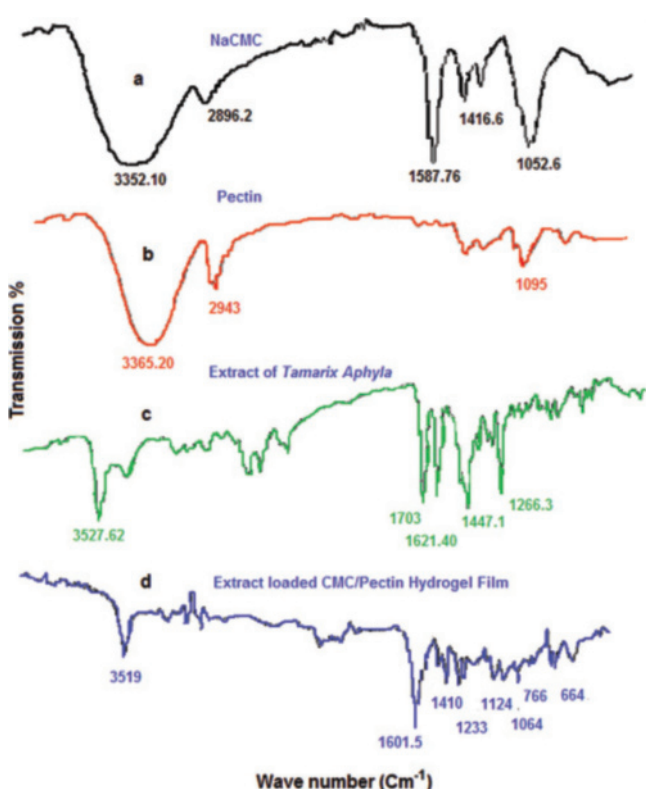


FIGURE 4. (a) FTIR analysis of NaCMC. (b) Pectin. (c) Extract. (d) Hydrogel film.

2943 cm^{-1} , that was hydroxyl group (OH) and alkyl chain (C-H) stretching vibration. The peaks at 1095 cm^{-1} could be assigned to $-\text{CH}-\text{O}-\text{CH}-$ stretching (Akhlaj and Mohammed, 2011). Fig. 4c showed the ethanolic extract of *T. aphylla*. There are various characteristic peaks that

appeared in the extract, such as 3527.62 cm^{-1} , 1703 cm^{-1} , 1621 cm^{-1} , 1447.1 cm^{-1} , 1266.3 cm^{-1} assigning hydroxyl group, carboxylic functional group, aromaticity, alkyl, and ether chain derivatives, respectively (Wilpiszewska *et al.*, 2015). Fig. 4d displayed extract loaded CMC/Pectin hydrogel film formulation. A mixed pattern of peaks observed in extract-loaded CMC/Pectin hydrogel film, which ultimately exhibits the peaks of polymers (Na-CMC and Pectin) and active ethanolic extract of *T. aphylla*. The peaks at 3519 cm^{-1} specified hydrophilic functional group (O-H) or N-H functional group. The characteristic band at 1601.5 cm^{-1} was representing the amide-I band of the amide group. The peak at 1410 cm^{-1} and 1233 cm^{-1} assigned C-H stretching of the CH_2 group. The peak at 1124 cm^{-1} indicated O-H vibrating band, 1064 cm^{-1} suggested the confirmation of secondary alcohol ($-\text{CH}-\text{OH}$ in cyclic alcohol C-O stretch). The overall results clearly suggested that ethanolic extract of *T. aphylla* successfully incorporated into CMC/pectin hydrogel formulations, and there is no polymer extract interaction that appears in the results (Ballesteros *et al.*, 2018).

Scanning electron microscopy

Scanning electron microscopy of the prepared polymeric film loaded with the *T. aphylla* extract was performed in order to study the morphology of the films. The scanning electron microscopy images of the prepared film clearly showed voids in the structure, as shown in Figs. 5a and 5b. This confirms the formation of highly porous films. The porous structure is important for the hydrophilicity of the films because water can penetrate through these voids in the polymeric structure (Barkat *et al.*, 2020). Two images (Figs. 5a and 5b) were taken from an electron microscope. Fig. 5a

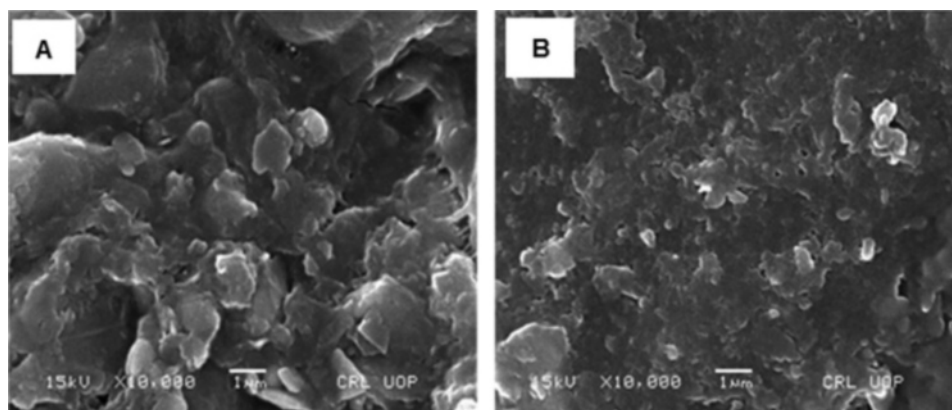


FIGURE 5. (a) SEM image of blank hydrogel film and (b) *T. aphylla* extract loaded hydrogel film. Specific acceleration voltage was 30 kV, and magnification power was 50 \times .

shows the blank CMC/Pectin hydrogel film, while Fig. 5b represents *T. aphylla* bark extract loaded hydrogel film. SEM images displayed the porous nature of films that have a slightly rough surface. In hydrogel formulation, citric acid tightly cross-linked polymeric chain and then arranged the chains in a specific manner to produce void spaces between them (Jalil *et al.*, 2017). When these chains come in contact with water, it filled these spaces and caused higher swelling of the polymeric network, which is beneficial for wound dressing material (Rachtanapun *et al.*, 2012). Fig. 5b exhibited that spaces between polymeric networks effectively accommodated *T. aphylla* extract and represents a better combination with the polymer matrix. This result was supported by Yang *et al.*'s study. They designed polyvinyl Alcohol and chitosan base hydrogel and evaluate its antimicrobial and antioxidant activities. The SEM was done and exhibited that hydrogel has a porous structure that has a close resemblance to honeycomb. The rough and porous nature of the hydrogel membrane has maximum water uptake capacity, which provides excellent water availability in the hydrogel amorphous region.

Drug content determination

Drug content of different hydrogel formulations was determined using a UV-Visible spectrophotometer. Drug content gives information regarding the uniform and homogenous distribution of drugs present in the pharmaceutical dosage forms (Ortega-Toro *et al.*, 2014). Tab. 2 presented the value of drug content of formulations A3, E3, and S3. The drug content of A3 was $85 \pm 0.1\%$, which was the highest from the other two formulations (E3 and S3). E3 showed a drug content of about $82.5 \pm 0.4\%$, and S3 exhibited about $80 \pm 0.3\%$. All these CMC/Pectin hydrogel films formulation shows a higher drug content,

TABLE 2

Drug content percentage of CMC/Pectin hydrogel films

S. No.	Drug required (μg)	Drug obtained ($\mu\text{g} \pm \text{SD}$)	% Drug content $\pm \text{SD}$
A3	200	170 ± 0.5	85.0 ± 0.1
E3	200	165 ± 0.9	82.5 ± 0.4
S3	200	160 ± 0.4	80.0 ± 0.3

which confirmed the actual presence of the drug in the hydrogel formulation.

Weight uniformity

The weight of CMC/Pectin hydrogel film was analyzed in mg, and the average and standard deviation were calculated. The weight of hydrogel film ranged from 0.24 ± 0.25 to 0.3 ± 0.07 . The Student's *t*-test was applied to data, which showed that there was no significant difference ($P > 0.05$) between hydrogel film formulations. All formulations were dried at the same temperature, which causes an equal amount of water or moisture loss from the hydrogel. As a result, all the formulations possess uniform weight. Values of weight uniformity and physical appearance of the hydrogel are presented in Tab. 3.

In vitro drug release studies

The release of drug from pharmaceutical dosage form is important for therapeutic efficacy (Khan *et al.*, 2020). For this purpose, drug release from the prepared hydrogel films was conducted. Fig. 6 shows the % accumulative *in vitro* drug release pattern. On the basis of drug content, three formulations (A3, E3 and S3) were selected and subjected to *in vitro* drug release studies. The drug released from hydrogel was estimated at times 0, 1, 2, 3, 4, and up to 24 h, and the percentage of accumulative drug release was

TABLE 3

Weight uniformity and physical appearance of CMC/pectin hydrogel films

Serial No.	Weight uniformity (mg)	Physical appearance
A1	0.29 ± 0.06	Hard and less flexible
A2	0.28 ± 0.11	Smooth and less flexible
A3	0.3 ± 0.07	Smooth and elastic
E1	0.25 ± 0.05	Brittle and rough
E2	0.22 ± 0.03	Smooth and elastic
E3	0.3 ± 0.8	Smooth and elastic
S1	0.24 ± 0.25	Smooth and elastic
S2	0.26 ± 0.01	Hard and rough
S3	0.28 ± 0.08	Tough and elastic

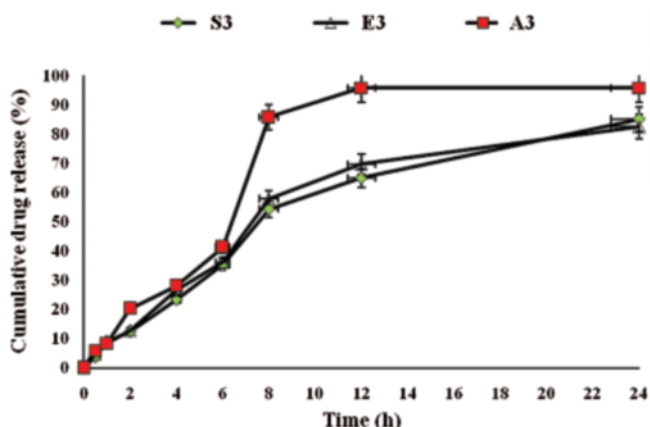


FIGURE 6. Accumulative drug release from CMC/Pectin hydrogel films formulations. The data were represented as mean \pm SD and analyzed using ANOVA. $P < 0.05$ refers to the statistical significance of formulation A3 and E3 from S3 formulation.

recorded. A3 and E3 showed significantly highest ($P < 0.05$) drug release as compared to S3 formulation. This was directly related to the swelling behavior of hydrogel film (Jalil *et al.*, 2017). A3 and E3 having a maximum amount of Na-CMC and pectin, respectively, both are hydrophilic in nature, so when coming in contact with the medium, readily swelled and pores are developed in hydrogel film, which causes a slow release of drug from the formulation. Another reason for slow drug release was that the recipient solution becomes saturated, and the amount of drug in the hydrogel

became less. S3 formulation exhibited the lowest drug release and it was due to the high concentration of citric acid, which forms a compact structure and causes less swelling of hydrogel. As a result, slow dissolution of the drug presented the slow diffusion and ultimately low quantity of drug release from S3 formulation. All samples first showed burst release due to accumulation of extract at the surface of CMC/Pectin hydrogel film during the drying process, so it releases faster, and then release becomes sustained (Ali *et al.*, 2018).

Kinetic model

The drug release mechanism (*T. apophylla* extract) from CMC/Pectin hydrogel film was evaluated by plotting release data in Weibull kinetic model as shown in Fig. 7. Three formulations A3, E3, and S3 exhibited almost the same release mechanism, and data depicted that hydrogel follows the reports of Burki *et al.* (2020) In Wei-bull kinetics, the value of “b” explored the pattern of drug release. The “b” value for the A3 formulation was less than 1 ($b < 1$) (A3: $b = 0.878$, $r^2 = 0.978$), which depicted that rapid erosion of the polymeric network causes an early release of the drug in about 6 h. While formulation E3 and S3 show delayed release of drug with sigmoidal curve having b value greater than ($b > 1$) (E3: $b = 1.089$, $r^2 = 0.998$) and (S3: $b = 1.121$, $r^2 = 0.969$). This demonstrated the tighten the polymeric structure which causes constriction of the polymeric chain resulting in controlled release of the drug for a prolonged period (24 h) of time. The release behavior was non-Fickian/Zero-order.

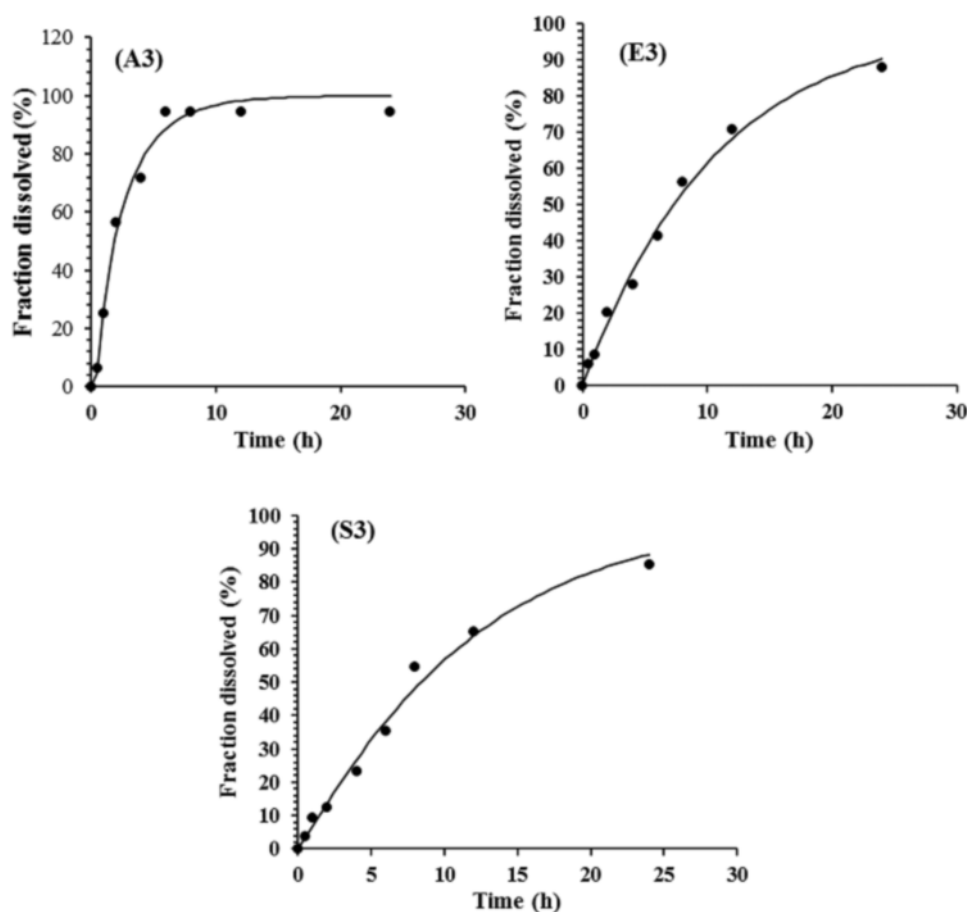


FIGURE 7. Formulation A3, E3 and S3 of CMC/Pectin Hydrogel film showing release profile.

*In vivo study**Wound size measurement*

Wound healing is a natural process obtained through four highly programmed stages: hemostasis, inflammation, proliferation, and remodeling. For a wound to be healed effectively, all these stages must occur in the appropriate sequence and time frame (Okur *et al.*, 2019; Ayla *et al.*, 2019). Healing involves platelet aggregation, blood clotting, the formation of fibrin, a response of inflammation to injury, alteration in the ground substances, angiogenesis, and re-epithelialization (Mehmet *et al.*, 2020b).

Three groups of rabbits (male) were used for determining the wound healing activity of *T. aphylla* extract incorporated into CMC/Pectin hydrogel film. The percentage of wound closure of the experimental group, standard group, and control group is presented in Tab. 4 and Fig. 8, showing the

burn wounds before treatment, during treatment, and after the treatment for various groups. Rabbits in the experimental group were treated with *T. aphylla* bark extract loaded hydrogel film, and their wound size reduction at day 7 was 60.58%, at day 14 was 80.69% and at day 21 was 90.76%. Rabbits in the standard group were treated with Euflavin (Bernol® cream), and the percent wound closure was 65.31% at day 7, 82.47% at day 14, and 95.54% at day 21. In the control group, rabbits were treated with blank hydrogel. The rate of wound contractions was examined at day 7, day 14, and day 21, which were 35.36%, 45.90%, and 52.49%, respectively. By comparing and analyzing the results of all groups, there is a significant difference ($P < 0.05$) between the control group and the experimental group. While there is no significant difference in percent wound closure of the experimental group and standard group ($P > 0.05$).

TABLE 4

Wound contraction percentage of experimental, standard and blank group

Groups	Day 7 (mean \pm SD) mm ²	Day 14 (mean \pm SD) mm ²	Day 21 (mean \pm SD) mm ²
Experimental group	60.58 \pm 0675	80.69 \pm 435	90.76 \pm 0813
Standard group	65.31 \pm 2.89	82.47 \pm 1.76	95.54 \pm 0954
Control group	35.36 \pm 0.85	45.90 \pm 0.74	52.49 \pm 1.26

Note: All the values are presented as mean \pm SD.

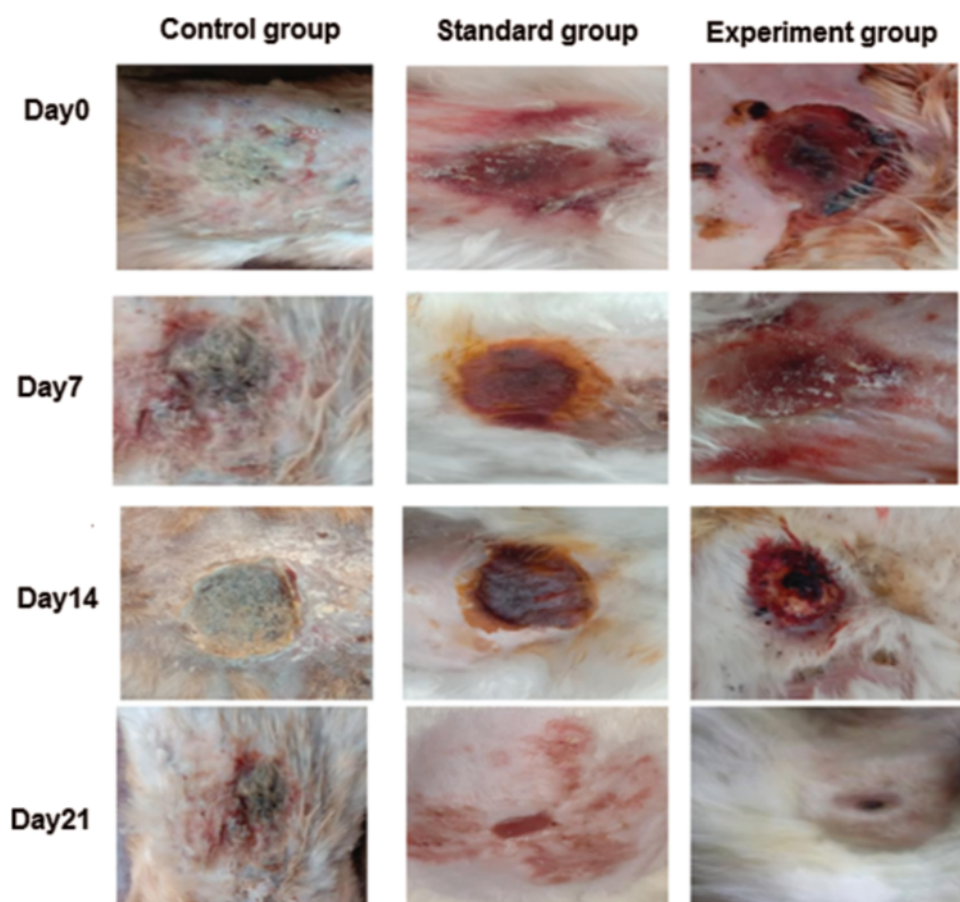


FIGURE 8. Wound closure of control, standard and experimental rabbits at Day0, Day7, Day14 and Day21.

This significant difference depicted that the rate of wound healing and percent re-epithelialization was faster in the experimental group as compared to the control group. It clearly indicated that *T. aphylla* bark extract contained various active constituents that are responsible for faster burn wound healing activity like Bernol[®] cream. Yusufoglu and Alqasoumi (2011) utilized ethanolic extract of *T. aphylla* for investigation of its potential anti-inflammatory, radical scavenging, and wound healing efficacy. Sajid et al. (2019) interrogated wound healing efficacy in animals by applying an ethanolic extract of *T. aphylla*. Treated animals that have been cured with the extract showed significant antibacterial activity as compared to the market preparation. The percentage of collagen deposition in the extract-treated group was 93.86%. Tensile strength was enhanced as compared to standard market preparation. 40% reduction was observed in the epithelialization period of the treated wounds (Sajid et al., 2019).

Histopathology of wounds

Wound healing occurs through overt overlapping phases: hemostasis, inflammation, proliferation, and remodeling. During the inflammation phase, to protect against the invading microbes, neutrophils are catalyzed, and proteases and reactive oxygen species (ROS) are released at the wound site. However, the overproduction of ROS could impede the wound healing process because it could give rise to serious damage of the cells such as fibroblasts which secretes collagen and glycosaminoglycans that are beneficial to tissue structure remodeling for wound repair (Xian et al., 2020;

Zhang et al., 2020). The Na-CMC/Pectin hydrogel film was found to be effective in burn wound healing applied topically and its pharmacodynamics effect was comparable to the standard marketed product (Burnol[®]) in the experimental group as compared to the control group. The hydrogel showed its action by stimulating the synthesis of collagen which has been reported to be a vital stage of wound healing. In the histopathological evaluation, fibroblast proliferation was also found accompanied by neovascularization in both experimental (Hydrogel treated) and standard group (Figs. 9b and 9c). Healing of wounds in any tissues follows a predictable sequence of events with the objective to restore damaged tissues as closely as possible to the normal condition (Ashraf et al., 2018; Khan et al., 2020). The current study clearly indicated that *T. aphylla* loaded hydrogel film boosts the proliferation and remodeling stages in the healing of wounds.

Biochemical study

Hydroxyproline is an amino acid that is found in the collagen in abundance. It is considered a key for collagen content. Hydroxyproline accelerates collagen formation, which strengthens the wound tissues (Elegbede et al., 2020). Similarly, hexosamine, which is a component of glycosaminoglycans, helps in the stabilization of collagen fibers. The results of the biochemical analysis have been shown in the Figs. 10a and 10b. The experimental and standard groups significantly enhanced the hydroxyproline content level in the wound tissues as compared to the control group. The level of hydroxyproline in control,

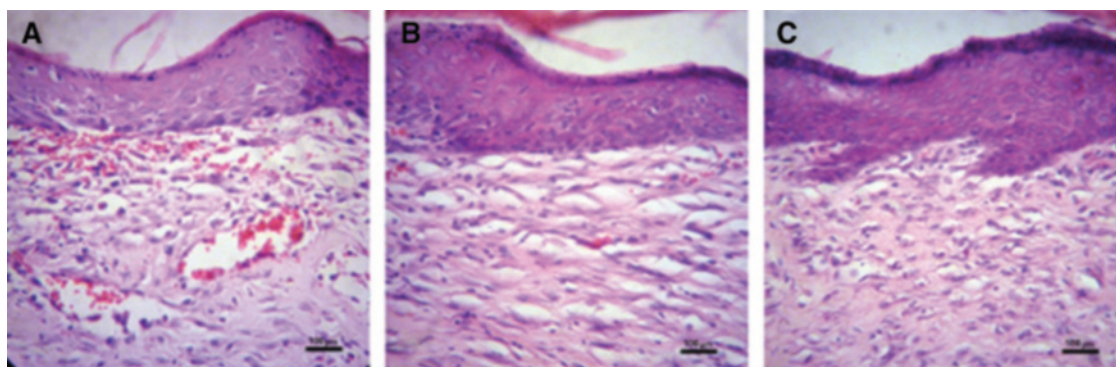


FIGURE 9. Histopathological evaluation of wound tissues of (a) control group (b) experimental group and (c) standard group after 21 days. Original magnification 400 \times (the scale bar is 100 μ m).

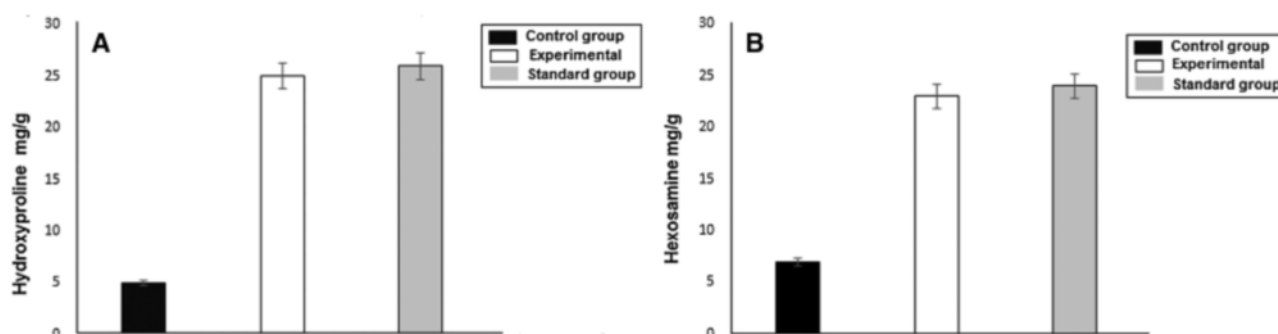


FIGURE 10. (a) Hydroxyproline level in control, experimental and standard group. (b) Hexosamine level in control, experimental and standard groups.

experimental, and standard groups were 5, 25, and 26 mg/g, respectively. This difference indicates the faster healing of wounds in these two groups relative to the control. The hexosamine level in control, experimental and standard groups were 7, 23, and 24 mg/g, respectively, which suggested the improvement of stabilized collagen fibers in burn wound tissues. Hydroxyproline is an amino acid that is found in the collagen in abundance. It is considered a key for collagen content. Hydroxyproline accelerates collagen formation, which strengthens the wound tissues (Elegbede *et al.*, 2020). Similarly, hexosamine, which is a component of glycosaminoglycans, helps in the stabilization of collagen fibers. The results of the biochemical analysis have been shown in the Figs. 10a and 10b. The experimental and standard groups significantly enhanced the hydroxyproline content level in the wound tissues as compared to the control group. The level of hydroxyproline in control, experimental, and standard groups were 5, 25, and 26 mg/g, respectively. This difference indicates the faster healing of wounds in these two groups relative to the control. The hexosamine level in control, experimental and standard groups were 7, 23, and 24 mg/g, respectively, which suggested the improvement of stabilized collagen fibers in burn wound tissues.

Conclusions

CMC/Pectin hydrogel film was fabricated successfully, which exhibited a smooth and elastic appearance, exudates absorbing and drug release properties. The animal study predicted excellent wound healing properties that verify the use of *T. aphylla* extract for burn wounds healing purposes. Overall, the prepared hydrogel films exhibited an accelerated wound healing process, more organized tissue formation, and collagen deposition at the wound site. Moreover, studies need to be conducted for isolation/purification of constituents and then formulating hydrogel of the isolated constituent.

Acknowledgement: We are thankful to Dr. Nauman Rahim Khan (Lecturer at Faculty of Pharmacy, Gomal University, D. I. Khan, Pakistan) for helping us in FTIR analysis and Braga (Professor at Center of Biotechnology, Federal University of Paraiba, Brazil), who conducted the histopathological and biochemical analyses.

Availability of Data and Materials: It can be obtained from the corresponding author on request.

Authors' Contribution: BAK designed and supervised the study plan. FK performed all the experiments. MKK helped in formulation development and writing of the manuscript. SUK and FH edited the manuscript and did the formal analysis. All authors have read and approved the manuscript.

Ethical Approval: All the animals in the study were handled and used according to the guidelines approved by the Gomal University Ethical Review Board (ERB) under Reference No. (ERB/GU-14-2019).

Funding Statement: The authors received no specific funding for this study.

Conflicts of Interest: The authors declare that they have no conflicts of interest to report regarding the present study.

References

- Akhlaq M, Mohammed A (2011). New phenolic acids from the galls of *Tamarix aphylla* (L.) Karst. *International Research Journal Pharmacy* **4**: 222–225.
- Alam P, Ansari MJ, Anwer MK, Raish M, Kamal YK, Shakeel F (2017). Wound healing effects of nanoemulsion containing clove essential oil. *Artificial Cells, Nanomedicine, and Biotechnology* **45**: 591–559.
- Alhourani N, Kasabri V, Bustanji Y, Abbassi R, Hudaib M (2018). Potential antiproliferative activity and evaluation of essential oil composition of the aerial parts of *Tamarix aphylla* (L.) H. Karst.: A wild grown medicinal plant in Jordan. *Evidence-Based Complementary and Alternative Medicine* **2018**: 9363868.
- Ali M, Hussain Z, Basit HM, Mahmood S, Ullah N (2018). Novel composite pH controlled drug release hydrogel containing dexibuprofen. *RADS Journal of Pharmacy and Pharmaceutical Sciences* **6**: 223–235.
- Annabi N, Ali TJJ, Mohsen A, Luiz B, Chaenyung C, Gulden C, Mehmet RD, Nicholas A, Ali K (2014). 25th anniversary article: Rational design and applications of hydrogels in regenerative medicine. *Advances in Materials* **26**: 85–124.
- Ashraf UK, Muhammad ZU, Ruqqaya A, Hina R, Sidra K, Hadayat U, Hussain A, Shakir DA, Yeong SK, Salman K (2018). Antinociceptive properties of 25-methoxy hispidol A, a triterpenoid isolated from *Poncirus trifoliata* (Rutaceae) through inhibition of NF- κ B signalling in mice. *Phytotherapy Research* **33**: 327–341.
- Ayla S, Okur ME, Günel MY, Özdemir EM, Çiçek PD, Yoltaş A, Biçeroğlu Ö, Karahüseyinoğlu S (2019). Wound healing effects of methanol extract of *Laurocerasus officinalis* roem. *Biotechnology and Histochemistry* **94**: 180–188. DOI 10.1080/10520295.2018.1539242.
- Ballesteros LF, Cerqueira MA, Teixeira JA, Mussatto SI (2018). Production and physicochemical properties of carboxymethyl cellulose films enriched with spent coffee grounds polysaccharides. *International Journal of Biological Macromolecules* **106**: 647–655.
- Bao Y, Ma J, Li N (2011). Synthesis and swelling behaviors of sodium carboxymethyl cellulose-g-poly (AA-co-AM-co-AMPS)/MMT superabsorbent hydrogel. *Carbohydrate Polymers* **84**: 76–82.
- Barkat AK, Afnan K, Muhammad KK, Valdir AB (2020). Preparation and properties of high sheared poly(vinyl alcohol)/chitosan blended hydrogels films with *Lawsonia inermis* extract as wound dressing. *Journal of Drug Delivery Science and Technology* **61**: 2021. DOI 10.1016/j.jddst.2020.102227.
- Bibi S, Afzal M, Aziz N, Din BU, Khan MY, Khan A, Komal H (2015). Antifungal activity of *Tamarix aphylla* (L.) Karst. stem-bark extract against some pathogenic fungi. *American-Eurasian Journal of Agricultural & Environmental Science* **15**: 541–545.
- Burki IK, Khan MK, Khan BA, Uzair B, Braga VA, Jamil QA (2020). Formulation development, characterization, and evaluation of a novel dexibuprofen-capsaicin skin emulgel with improved *in vivo* anti-inflammatory and analgesic effects. *AAPS PharmSciTech* **21**: 211. DOI 10.1208/s12249-020-01760-7.

- Caló E, Khutoryanskiy VV (2015). Biomedical applications of hydrogels: A review of patents and commercial products. *European Polymer Journal* **65**: 252–267.
- Díez-Pascual AM, Díez-Vicente AL (2015). Wound healing bionanocomposites based on castor oil polymeric films reinforced with chitosan modified ZnO nanoparticles. *Biomacromolecules* **16**: 2631–2644.
- Ebid AI (2015). Anti-bacterial activity of folk medicinal plant extracts of Saudi Arabia on isolated bacteria. *Journal of Applied Life Sciences International* **3**: 49–54.
- Elegbede RD, Ilomuanya MO, Sowemimo AA, Nneji A, Joubert E, de Beer D, Koekemoer T, van DV (2020). Effect of fermented and green *Aspalathus linearis* extract loaded hydrogel on surgical wound healing in Sprague Dawley rats. *Wound Medicine* **29**: 100186.
- Ghorpade VS, Yadav AV, Dias RJ (2017). Citric acid crosslinked cyclodextrin/carboxymethylcellulose hydrogel films for controlled delivery of poorly soluble drugs. *Carbohydrate Polymers* **164**: 339–348.
- Girard D, Laverdet B, Buhe V, Trouillas M, Ghazi K, Alexaline MM, Egles C, Misery L, Coulomb B, Lataillade JJ, Berthod F, Desmoulière A (2007). Biotechnological management of skin burn injuries: Challenges and perspectives in wound healing and sensory recovery. *Tissue Engineering Part B: Reviews* **23**: 59–82.
- Han Z, Yin, W, Zhang J, Niu S, Ren L (2013). Active anti-erosion protection strategy in Tamarisk (*Tamarix aphylla*). *Scientific reports* **3**: 3429.
- Hemant KN, Srivastava AK, Srivastava R, Kurmi ML, Chandel HS, Ranawat MS (2016). Pharmacological investigation of the wound healing activity of *Cestrum nocturnum* (L.) ointment in Wistar albino rats. *Journal of Pharmaceutics* **2016**: 760–770.
- Hoffman AS (2012). Hydrogels for biomedical applications. *Advances in Drug Delivery* **64**: 18–23.
- Huang J, Chen L, Gu Z, Wu J (2019a). Red Jujube-incorporated gelatin methacryloyl (GelMA) hydrogels with anti-oxidation and immunoregulation activity for wound healing. *Journal of Biomedical and Nanotechnology* **15**: 1357–1370.
- Huang J, Chen L, Yuan Q, Gu Z, Wu J (2019b). Tofu-based hybrid hydrogels with antioxidant and low immunogenicity activity for enhanced wound healing. *Journal of Biomedical Nanotechnology* **15**: 1371–1383.
- Jalil A, Khan S, Naeem F, Haider MS, Sarwar S, Riaz A, Ranjha NM (2017). The structural, morphological and thermal properties of grafted pH sensitive interpenetrating highly porous polymeric composites of sodium alginate/acrylic acid copolymers for controlled delivery of diclofenac potassium. *Designed Monomers and Polymers* **20**: 308–324.
- Jasim T, Albazaz H (2019). *Tamarix aphylla* L.: A review. *Research Journal of Pharmacy and Technology* **12**: 3219–3222. DOI 10.5958/0974-360X.2019.00541.9.
- Kased RF, Amer RI, Attia D, Elmazar MM (2017). Honey-based hydrogel: *In vitro* and comparative *in vivo* evaluation for burn wound healing. *Scientific Reports* **7**: 9692.
- Khan BA, Shahid U, Muhammad KK, Bushra U, Farid M, Valdir AB (2020). Fabrication, physical characterizations and *in vitro*, *in vivo* evaluation of ginger extract-loaded gelatin/poly(vinyl alcohol) hydrogel films against burn wound healing in animal model. *AAPS PharmSciTech* **21**: 323. DOI 10.1208/s12249-020-01866-y.
- Kibar EA, Us F (2013). Thermal, mechanical and water adsorption properties of corn starch-carboxymethylcellulose/methylcellulose biodegradable films. *Journal of Food Engineering* **114**: 123–131.
- Liu H, Wang CY, Li C, Qin YG, Wang ZH, Yang F, Li ZH, Wang JC (2018). A functional chitosan-based hydrogel as a wound dressing and drug delivery system in the treatment of wound healing. *RSC Advances* **8**: 7533–7549.
- Martelli SM, Motta C, Caon T, Alberton J, Bellettini IC, Soldi V (2017). Edible carboxymethyl cellulose films containing natural antioxidant and surfactants: α -tocopherol stability, *in vitro* release and film properties. *LWT—Food Science and Technology* **77**: 21–29.
- Mehmet EO, Şule A, Vildan Y, Neşe BA, Ayşegül Y, Duygu O, Hande S, Neslihan UO (2020a). Evaluation of burn wound healing activity of novel fusidic acid loaded microemulsion based gel in male Wistar albino rats. *Saudi Pharmaceutical Journal* **28**: 338–348.
- Mehmet EO, Şule A, Vildan Y, Neşe BA, Ayşegül Y, Duygu O, Hande S, Neslihan UO (2020b). Evaluation of burn wound healing activity of novel fusidic acid loaded microemulsion based gel in alginate-carboxymethylcellulose blend films. *Food Research International* **41**: 1007–1014.
- Mishra RK, Datt M, Banthia AK (2008). Synthesis and characterization of pectin/PVP hydrogel membranes for drug delivery system. *AAPS PharmSciTech* **9**: 395–403.
- Okur ME, Karantas ID, Şenyiğit Z, Okur NÜ, Okurd PS (2019). Recent trends on wound management: New therapeutic choices based on polymeric carriers. *Asian Journal of Pharmaceutical Sciences* **15**: 661–684. DOI 10.1016/j.ajps.2019.11.008.
- Ortega-Toro R, Jiménez A, Talens P, Chiralt A (2014). Food hydrocolloids effect of the incorporation of surfactants on the physical properties of corn starch films. *Food Hydrocolloids* **38**: 66–75.
- Peck M, Molnar J, Swart D (2009). A global plan for burn prevention and care. *Bulletin of the World Health Organization* **87**: 802–803.
- Rachtanapun P, Luangkamin S, Tanprasert K, Suriyatem R (2012). Carboxymethyl cellulose film from durian rind. *LWT—Food Science and Technology* **48**: 52–58.
- Ramli NA, Wong TW (2011). Physicochemical effects on partial thickness wound healing. *International Journal of Pharmaceutics* **403**: 73–82.
- Sajid A, Alam S, Ahmad S, Ali M, Ahsan W, Siddiqui MR, Ansari S, Shamim S, Ali MD (2019). Wound healing activity of alcoholic extract of *tamarix aphylla* l. on animal models. *Biomedical and Pharmacology Journal* **12**: 41–48.
- Sutar PB, Mishra RK, Pal K, Banthia AK (2008). Development of pH sensitive polyacrylamide grafted pectin hydrogel for controlled drug delivery system. *Journal of Materials Science: Materials in Medicine* **19**: 2247–2253.
- Tong Q, Xiao Q, Lim LT (2008). Preparation and properties of pullulan-alginate-carboxymethylcellulose blend films. *Food Research International* **41**: 1007–1014.
- Towfiq A, Hamza AS, Munahi A (2015). The effect of Henna (*Lawsonia inermis*) on the wound healing of Local Arabian Horses. *Journal of Kerbala University* **13**: 78–91.
- Wilpiszewska K, Antosik AK, Szychaj T (2015). Novel hydrophilic carboxymethyl starch/montmorillonite nanocomposite films. *Carbohydrate Polymers* **128**: 82–89.
- Woessner JF, Jr (1961). The determination of hydroxyproline in tissue and protein samples containing small proportions of this amino acid. *Archives in Biochemical and Biophysics* **1961**: 93.

- Xian C, Gu Z, Liu G, Wu J (2020). Whole wheat flour coating with antioxidant property accelerates tissue remodeling for enhanced wound healing. *Chinese Chemical Letters* **31**: 1612–1615. DOI 10.1016/j.ccl.2019.09.011.
- Yusufoglu HS, Alqasoumi SI (2011). Anti-inflammatory and wound healing activities of herbal gel containing an antioxidant *Tamarix aphylla* leaf extract. *International Journal of Pharmacology* **7**: 829–835.
- Zhang S, Hou J, Yuan Q, Xin P, Cheng H, Gu Z, Wu J (2020). Arginine derivatives assist dopamine-hyaluronic acid hybrid hydrogels to have enhanced antioxidant activity for wound healing. *Chemical Engineering Journal* **392**: 123775. DOI 10.1016/j.cej.2019.123775.